



## Retrieval of crop biophysical parameters from Sentinel-2 remote sensing imagery



Qiaoyun Xie<sup>a</sup>, Jadu Dash<sup>b</sup>, Alfredo Huete<sup>a</sup>, Aihui Jiang<sup>c</sup>, Gaofei Yin<sup>d</sup>, Yanling Ding<sup>e</sup>, Dailiang Peng<sup>f,\*</sup>, Christopher C. Hall<sup>a</sup>, Luke Brown<sup>b</sup>, Yue Shi<sup>f</sup>, Huichun Ye<sup>f</sup>, Yingying Dong<sup>f</sup>, Wenjiang Huang<sup>f,\*</sup>

<sup>a</sup> University of Technology Sydney, Faculty of Science, Sydney NSW 2007, Australia

<sup>b</sup> University of Southampton, School of Geography and Environmental Science, Highfield, Southampton SO171BJ, UK

<sup>c</sup> Shandong Normal University, College of Geography and Environment, Jinan 250358, Shandong, China

<sup>d</sup> Faculty of Geosciences and Environmental Engineering, Southwest Jiaotong University, Chengdu 610031, China

<sup>e</sup> School of Geographical Sciences, Northeast Normal University, Changchun, 130024, China

<sup>f</sup> Key Laboratory of Digital Earth Science, Institute of Remote Sensing and Digital Earth, Chinese Academy of Sciences, Beijing 100094, China

### ARTICLE INFO

#### Keywords:

Leaf area index  
Chlorophyll content  
Artificial neural network  
Look-up table  
Vegetation index

### ABSTRACT

The red-edge bands place the recently available multispectral Sentinel-2 imagery at an advantage over other multispectral sensors, and hypothetically offer improved crop biophysical variable retrieval accuracy. In this study, Sentinel-2 data was tested for its ability to estimate winter wheat leaf area index (LAI), leaf chlorophyll content (LCC) and canopy chlorophyll content (CCC). Artificial neural network (ANN) and look-up table (LUT) (based on PROSAIL simulations) and vegetation index (VI) methods were applied to retrieve biophysical parameters, and compared with the biophysical processor module embedded in the Sentinel Application Platform (SNAP) software. Based on a set of in situ measurements (62 samples) and near-synchronous Sentinel-2 images, the inversion approaches were applied and validated. The results showed that: 1) Sentinel-2 red-edge bands improved the retrievals of chlorophyll / LAI compared to traditional VIs; 2) the red-edge VIs outperformed other approaches; and 3) the SNAP biophysical processor obtained comparable accuracies of LAI and CCC estimation compared to the ANN and LUT approaches, giving  $R^2$  values above 0.5 with relatively low RMSE ( $1.53 \text{ m}^2/\text{m}^2$  for LAI, and  $148.58 \mu\text{g}/\text{cm}^2$  for CCC). We recommend VI retrieval approach for small region with ground measurements, whereas where ground data is not available, SNAP is applicable for versatile and rapid winter wheat parameter estimation (though results need to be evaluated alongside the provided quality indicators). Summarizing, the results demonstrate the suitability of Sentinel-2 data, especially its red-edge bands, for crop biophysical variables retrieval. Future studies will need to make comparisons across canopy types to better assess the capability of the SNAP biophysical processor.

### 1. Introduction

The regular and accurate mapping of crop biophysical variables is essential in numerous applications such as precision agriculture, land surface monitoring, natural resource management, and hydrological modelling. Leaf area index (LAI), for example, can provide insight into the function and structure of the canopy; while the chlorophyll content is strongly related to leaf nitrogen content, and thus is a very good indicator of stress, such as nitrogen deficiency (Houlès et al., 2001). The chlorophyll content can be determined at the leaf level (leaf chlorophyll content, LCC), whilst it can be calculated at the canopy level (canopy

chlorophyll content, CCC) by multiplying the LCC and LAI. Some studies have suggested that these chlorophyll products could be of very high interest in primary production models because they are indicative of the photosynthetic efficiency (Green et al., 2003).

Traditional ground measurements of crop biophysical parameters are time consuming and labour-intensive, and usually conducted within small regions. A promising alternative is to use earth observation techniques for mapping these parameters at a large scale and high temporal frequency. Numerous approaches have been developed for the retrieval of crop biophysical variables from remote sensing data, which generally fall into two categories: the empirical approaches that

\* Corresponding author.

E-mail addresses: [pengdl@radi.ac.cn](mailto:pengdl@radi.ac.cn) (D. Peng), [huangwj@radi.ac.cn](mailto:huangwj@radi.ac.cn) (W. Huang).

<https://doi.org/10.1016/j.jag.2019.04.019>

Received 30 January 2019; Received in revised form 24 April 2019; Accepted 25 April 2019

Available online 01 May 2019

0303-2434/ © 2019 Elsevier B.V. All rights reserved.

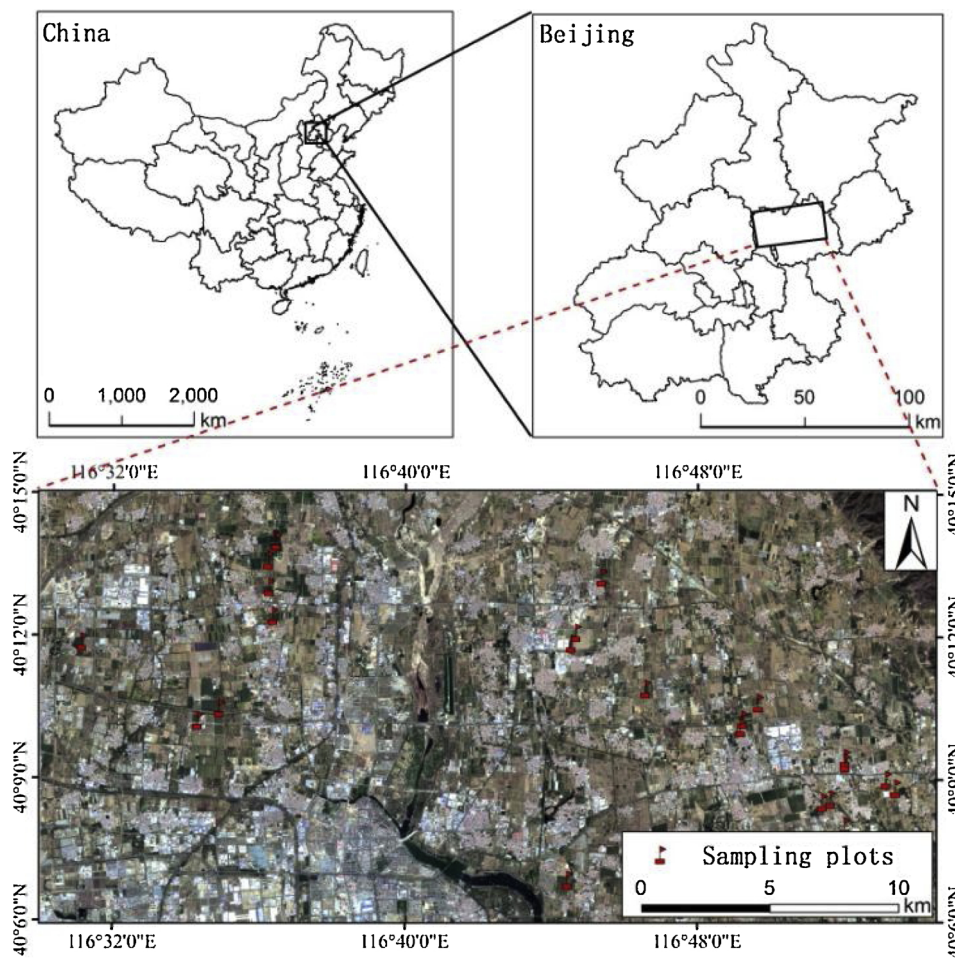


Fig. 1. Location of the field test sites in Shunyi District, Beijing, China. Also shown are the locations of the field plots where crop LAI measurements took place. The image is a false colour composite image from Sentinel-2 collected on 10 April 2016.

establish statistical regression models between the remote sensing data and field measurements (Kira et al., 2016; Pu and Cheng, 2015), and physical modelling approaches that use radiative transfer models (RTMs) to simulate the canopy spectral reflectance, and then invert the RTMs to obtain the sought parameters (Campos-Taberner et al., 2016; Féret et al., 2017).

For the first approach, the most frequently used model are vegetation indices (VIs) that contrast specific spectral characteristics of vegetation, for it is operationally and computationally simple to use. Many studies have demonstrated the successful application of this approach on various vegetation canopies (Darvishzadeh et al., 2008a,b; Kross et al., 2015; Nguy-Robertson et al., 2012; Viña et al., 2011; Xie et al., 2014). Despite the wide use of empirical techniques, their main disadvantage is that they are not reliable across different sites and crop types, and are hence less appropriate for regular mapping over large areas (Baret and Buis, 2008; Combal et al., 2003). For the physical modelling approach, differences in crop architecture, illumination, soil backgrounds, and viewing geometries can be accounted for by the RTM model, making it usable across multiple operational applications for retrieval of crop biophysical parameters (Bacour et al., 2006). Various physical modelling approaches have demonstrated strong potential for biophysical parameter estimation, such as artificial neural network and look-up table (Verrelst et al., 2012, 2014). Notwithstanding, there are still limitations to these methods, such as high computational demand and the need for proper parameterization. In addition, large differences in RTM parameters may result in limited variability in simulated spectra data, resulting in the ill-posed inversion problem during the variable retrieval (Atzberger, 2004).

Apart from modelling techniques, the potential of high temporal-spatial-spectral earth observation data to map crop biophysical variables has been shown by many studies (Claverie et al., 2013; Kross et al., 2015). Sentinel-2 was designed to enable continuity of multi-spectral data like Landsat and Satellite Pour l'Observation de la Terre (SPOT), and built upon the ESA MEdium Resolution Imaging Spectrometer (MERIS) heritage and successful experience with the NASA MODerate-resolution Imaging Spectroradiometer (MODIS) sensors in providing more spectral bands than Landsat and SPOT (Frampton et al., 2013). To serve the objectives of the European Earth Observation Programme "Copernicus", ESA's Sentinel-2 mission is aimed to provide data for the generation of high-level operational products such as land-cover, land use change detection, and mapping of geophysical variables.

The Sentinel-2 mission further improves the temporal, spatial and spectral resolution of remote sensing data, compared to other multi-spectral missions, such as Landsat, and offers great opportunities for vegetation monitoring. The Sentinel-2 bands, especially the two red-edge bands centred at 705 nm and 750 nm, have attracted the interest of many researchers. Although some studies have demonstrated the utility of Sentinel-2 data for vegetation monitoring (Battude et al., 2016; Verrelst et al., 2015b), comparative assessment of physical and empirical estimation techniques, particularly the newly embedded biophysical processor (based on the ANN method) in the Sentinel Application Platform (SNAP) software, which gives immediate retrieval results from Sentinel-2 images, has yet to be conducted. The objectives of this study are to: 1) Evaluate the potential of Sentinel-2 imagery, especially its red-edge bands, for winter wheat leaf area index, leaf

chlorophyll content and canopy chlorophyll content estimation; 2) Validate the estimation performance of the generic ANN algorithm embedded in the SNAP biophysical processor against the ground measurements, and compare it with other methods including empirically based VI models, and physically based ANN models with structural parameters optimized to this specific case and LUT approach.

## 2. Data collection

### 2.1. Field campaign

The data used in this study encompasses satellite acquisitions and ground measurement campaigns in Shunyi District, Beijing, China (40°00′–40°18′N, 116°28′–116°58′E) (Fig. 1), one of the largest agricultural areas in suburban Beijing. The area is dominated by winter wheat with an average field size of about 3 ha. During the winter wheat growing season in 2016 (seeded in 2015), three field campaigns were conducted on April 7 (jointing stage), April 20 (jointing stage) and May 18 (filling stage) respectively, to collect biophysical and biochemical parameters including leaf area index and chlorophyll content at both leaf and canopy level. A total number of 62 plots were measured, each covering an area of 1 m<sup>2</sup>, geolocated using a GPS device GPS RADIO-NOVA® RF Antenna Module with the accuracy of 2.5 m.

LAI measurements were carried out by using the Plant Canopy Analyzer instrument LAI-2200c (LI-COR Inc., Lincoln, NE, USA). The sensor does not account for the clumping effect, neither does it distinguish photosynthetically active leaf tissue from other plant elements, such as stems, senescent leaves or flowers (Darvishzadeh et al., 2008a,b). Thus, the LAI measured by LAI-2200c actually represents effective plant area index (PAI). For each 1 m<sup>2</sup> plot, the average value of LAI, generated from a set of 20 above and below canopy readings, was considered to be representative value for the respective plot. Because of the small plot size, we computed LAI without the outer ring to allow the minimum plot size to be 1.6 (instead of 3) times the canopy height. Additionally, a 45° view cap was used when measuring from the plot corners to prevent the sensor from seeing outside the plot area.

LCC measurements were conducted by laboratory analysis of the winter wheat leaves sampled in each 1 m<sup>2</sup> plot. Leaves that fully expanded and showed homogenous colour as well as no visible sign of damage were sampled from the top to the bottom of the canopy (Kong et al., 2017). Circular pieces of 0.25 cm<sup>2</sup> area were cut from each leaf and split into two parts. One part was used for dry weight determination, measured after the samples were dried in an oven at 70 °C for 48 h. The other part was first used for fresh weight measurement and then ground in 10 ml 80% acetone, before another 15 ml acetone was added to bring the final volume for each tube to 25 ml. All samples were placed in a cuvette and incubated in the dark at 25 °C for 48 h. The absorbance was then measured at 470 nm, 646 nm, and 663 nm wavelength using an L6 ultraviolet-visible spectrophotometer (INESA, China). Afterwards, the absorbance was used to compute chlorophyll *a* and *b* according to the method described in Gao research (2006). After the LCC and LAI were determined, the CCC was obtained by multiplying LCC with LAI for each plot.

### 2.2. Satellite data acquisition and processing

The Sentinel-2 mission consists of a pair of satellites, launched in 2015 and 2017, respectively. Each satellite delivers data every ten days, and taken together, they deliver data from all land surfaces and coastal zones at a frequency of every five days. Each satellite carries a Multi-Spectral Imager (MSI) with a swath width of 290 km, and provides data in 13 spectral bands spanning from the visible and near infrared region to the shortwave infrared region, including four bands at 10 m, six bands at 20 m and three bands at 60 m spatial resolution (Table 1) (Richter et al., 2012). In particular, Sentinel-2 incorporates two bands in the red-edge region, centred at 705 and 740 nm respectively.

Sentinel-2 images are free for download at the Copernicus Open Access Hub website (<https://scihub.copernicus.eu/>). In this study, we downloaded three cloud-free images taken on April 10, April 23 and May 13, corresponding to the field campaigns on April 7, April 20 and May 18 in 2016. The atmospheric correction of the Sentinel-2 images was performed using the Sen2cor atmospheric correction toolbox in the Sentinel Application Platform (SNAP) software (version 4.0). In order to preserve the red-edge region in the atmospherically corrected images, we chose 20 m as the spatial resolution during the atmospheric correction. The atmospherically corrected images then consisted of B2, B3, B4, B5, B6, B7, B8 A, B11, B12 (Table 1). The biophysical parameters LAI, LCC and CCC that we aimed to retrieve from Sentinel-2 mainly dominate the spectrum in visible and near infrared region, whilst wavebands in shortwave infrared region (B11 and B12) would not necessarily improve the estimation and were therefore excluded (Darvishzadeh et al., 2008a,b).

## 3. Methods

### 3.1. Radiative transfer modelling

The widely used PROSAIL model (Jacquemoud et al., 2009), a coupled model of the leaf model PROSPECT-4 (Feret et al., 2008) and the canopy model SAILH (Verhoef, 1984), was used to simulate canopy reflectance in this study. PROSPECT-4 simulates leaf reflectance and transmittance from 400 to 2500 nm, as a function of biochemistry and anatomical structure of the leaves. SAILH simulates top-of-canopy reflectance. The imposed range and distributions of the PROSAIL input variables are illustrated in Table 2. Of the input parameters, four parameters (leaf structural parameter, equivalent water thickness, dry matter content and sun zenith angle) were fixed. For the remaining input parameters (chlorophyll *a* + *b* content, LAI, average leaf angle, hot spot parameter and soil scaling factor), values were varied with the range obtained from the field campaigns and/or other studies focused on the same crop (Duveiller et al., 2011). Gaussian and uniform distributions were generated for input LCC and LAI respectively to put more emphasis on the variable values at the actual growth stages of winter wheat. 105,300 sets were generated randomly (all possible combinations of the input parameters) through the PROSAIL model. Two inversion approaches (ANN and LUT) were then used to derive biophysical variables using the RTM simulations and satellite data.

#### 3.1.1. Artificial neural network (ANN) based strategy

To set up the inversion, a synthetic dataset was established, in which the PROSAIL simulated spectrum reflectance was spectrally resampled according to the Sentinel-2 band configuration (B2, B3, B4, B5, B6, B7 and B8 A), and then used to train the network. We used a back-propagation ANN, which consists of an input layer, one or more hidden layers, and an output layer. The principle of training procedure is to learn the relationships between the input parameters (in our case the canopy reflectance bands) and the output parameters (in our case the LAI, LCC and CCC).

Generally, there are two steps to train the network: 1) a feed forward iteration to compute the output of the network; 2) a back-propagation learning rule to minimize the error between predicted outputs and input training values. For the ANN, the division of data for training, validation, testing was 70%, 15%, and 15% respectively. The training dataset was used for to update the weights and biases of the network, and the error of the test dataset was monitored during the training process (Vuolo et al., 2010). In order to optimize the structural parameters of the ANN for the network, we applied grid searching and varied both the momentum coefficient (MC) and learning rate (LR) from 0 to 1.0, at a step of 0.1. We also varied the number of nodes at each hidden layer from 4 to 7 (usually between nodes at the input layer and nodes at the output layer). Although setting up and training of the network is time consuming, once a network has been fully trained, the

**Table 1**  
Sentinel-2 MSI band settings.

Band	B1	B2	B3	B4	B5	B6	B7	B8	B8A	B9	B10	B11	B12
Band centre (nm)	443	490	560	665	705	740	783	842	865	945	1375	1610	2190
Band width (nm)	20	65	35	30	15	15	20	115	20	20	30	90	180
Spatial resolution (m)	60	10	10	10	20	20	20	10	20	60	60	20	20

latter retrieval of any variable can be accomplished immediately.

### 3.1.2. Look-up-table (LUT) based strategy

The LUT approach is a relatively simple inversion scheme, and has been applied to RTM data by many researchers to invert vegetation biophysical variables over various species and phenological stages (Darvishzadeh et al., 2008a,b; Vuolo et al., 2010). The synthetic dataset generated for the ANN approach was used to establish LUT, with a size of 10,000 parameter combinations. The estimation process is based on querying the LUT and applying a cost function that minimizes the summed differences between simulated and measured reflectance for all wavelengths (Verrelst et al., 2015a). In our study, the widely used root-mean-square error (RMSE) between the simulated and measured reflectance spectra was selected as the cost function. The final sought variable value was obtained by averaging the LUT variable combinations within 1% of the lowest RMSE value.

### 3.2. Empirical model: vegetation indices (VI)

In this study the performance of 12 VIs were investigated, including the Normalised Difference Vegetation Index (NDVI), Normalized Difference Vegetation Index Red-edge 1 (NDRE1), Normalized Difference Vegetation Index Red-edge 2 (NDRE2), Modified Simple Ratio (MSR), MERIS Terrestrial Chlorophyll Index (MTCI), Modified Chlorophyll Absorption Ratio Index (MCARI), Transformed Chlorophyll Absorption Reflectance Index/Optimized Soil-adjusted Vegetation Index (TCARI/OSAVI), TCARI/OSAVI [705,750], Modified Chlorophyll Absorption Ratio Index/Optimized Soil-adjusted Vegetation Index (MCARI/OSAVI), MCARI/OSAVI [705,750], Green Chlorophyll Index ( $CI_{green}$ ), Red-edge Chlorophyll Index ( $CI_{red-edge}$ ). The NDVI is the most widely used VI and plays a role as benchmark in plant parameter retrieval, whilst the NDRE1, NDRE2 and MSR were proposed to improve the saturation problem of the NDVI. Other indices used in our study were originally proposed for chlorophyll retrieval, but some studies have found that these VIs are also highly correlated with LAI (Delegido et al., 2013; Frampton et al., 2013). The formulae of the indices and the Sentinel-2 spectral bands used are provided in Table 3.

Relationships between the *in situ* crop variables (e.g. LAI, LCC and CCC) and each VI were established, and inter-comparison of the indices was performed by comparing the coefficients of determination ( $R^2$ ) of the calibration models. For each crop variable, the VI with the highest  $R^2$  was used to retrieve the sought variable.

**Table 2**  
Biophysical parameters chosen for PROSAIL model.

Parameter	Notes	Value	Distribution	Units	Number
<i>Leaf parameters</i>					
N	Leaf structural parameter	1.5	–	–	1
Cw	Equivalent water thickness	0.015	–	cm	1
Cm	Dry matter content	0.004	–	g/cm <sup>2</sup>	1
Cab	Chlorophyll a + b content	20*100	Gaussian standard deviation = 55, mean value = 50	µg/cm <sup>2</sup>	65
<i>Canopy parameters</i>					
LAI	Leaf area index	0.5*8.5	Uniform	m <sup>2</sup> /m <sup>2</sup>	60
ALA	Average leaf angle	35*70	Uniform	degree	3
hot	Hot spot parameter	0.05*0.5	Uniform	m/m	3
$\alpha_{soil}$	Soil scaling factor	0.5*1.2	Uniform	–	3
$\theta_s$	Sun zenith angle	45	–	degree	1

### 3.3. SNAP biophysical processor

The SNAP software, introduced in Section 2.2, was primarily developed to work with Sentinel series images. Since version 4.0, SNAP additionally provides a scientific processor named “Biophysical Processor” (in the “Thematic Land Processing” pull-down menu) for retrieval of LAI, CCC, canopy water content, fraction of photosynthetically active radiation absorbed by the green elements of the canopy and fraction of vegetation cover. The principle is to retrieve these parameters from Sentinel-2 instantaneous observations using an ANN approach. Based on a pre-trained neural net, the considered biophysical variables can be immediately retrieved for each pixel of the chosen Sentinel-2 image. The training data base is generated using an RTM, which should simulate within a good accuracy the canopy reflectance as observed within Sentinel-2 bands and geometry over most vegetation types and conditions that can be observed over the Earth.

Quantitative and qualitative quality indicators are attached to the SNAP biophysical product so that users can properly ‘weigh’ the data within its application according to the confidence they put on it, including:

- 1) Quality of top-of-atmosphere reflectance used as input, which corresponds to the previously produced indicators such as cloud occurrence, atmospheric correction and sensor problem.
- 2) Additional indicators based on:
  - Input out of range. This indicates that either there is problem with the input reflectance (e.g. cloud contamination, poor atmospheric correction or shadow), or that the retrieval algorithm produces unreliable results. When the input is out of range (fixed previously in the algorithm), the flag will be raised.
  - Output out of range. When the output appears to be out of the nominal range of variation (fixed previously in the algorithm), the flag will be raised.
  - Product uncertainty, which is a quantitative estimation of the uncertainty lies in the product.

### 3.4. Model validation

The performance of the estimation models was evaluated using the coefficient of determination ( $R^2$ ) and root-mean-square error (RMSE) when compared to field measurements. For the ANN, LUT and SNAP retrieval approaches, the retrieval results were directly compared with

**Table 3**  
A list of Vegetation Indices that have been analysed for use with Sentinel-2 using field data.

Index	Formulation	Bands used	Reference
NDVI	$\frac{\rho_{800} - \rho_{670}}{\rho_{800} + \rho_{670}}$	B7, B4	(Rouse et al., 1974)
NDRE1	$\frac{\rho_{750} - \rho_{705}}{\rho_{750} + \rho_{705}}$	B6, B5	(Gitelson and Merzlyak, 1994; Sims and Gamon, 2002)
NDRE2	$\frac{\rho_{790} - \rho_{720}}{\rho_{790} + \rho_{720}}$	B7, B5	(Barnes et al., 2000)
MSR	$\frac{(\rho_{800} / \rho_{670}) - 1}{\sqrt{(\rho_{800} / \rho_{670}) + 1}}$	B7, B4	(Chen, 1996)
MTCI	$\frac{\rho_{753.75} - \rho_{708.75}}{\rho_{708.75} + \rho_{681.25}}$	B7, B5, B4	(Dash and Curran, 2004)
MCARI	$[(\rho_{700} - \rho_{670}) - 0.2(\rho_{700} - \rho_{550})] * (\frac{\rho_{700}}{\rho_{670}})$	B5, B4, B3	(Daughtry et al., 2000)
TCARI/OSAVI	$\frac{3[(\rho_{700} - \rho_{670}) - 0.2(\rho_{700} - \rho_{550})(\rho_{700} / \rho_{670})]}{(1 + 0.16)(\rho_{800} - \rho_{670}) / (\rho_{800} + \rho_{670} + 0.16)}$	B7, B5, B4, B3	(Daughtry et al., 2000; Haboudane et al., 2002; Rondeaux et al., 1996)
TCARI/OSAVI [705,750]	$\frac{3[(\rho_{750} - \rho_{705}) - 0.2(\rho_{750} - \rho_{550})(\rho_{750} / \rho_{705})]}{(1 + 0.16)(\rho_{750} - \rho_{705}) / (\rho_{750} + \rho_{705} + 0.16)}$	B6, B5, B3	(Wu et al., 2008)
MCARI/OSAVI	$\frac{[(\rho_{700} - \rho_{670}) - 0.2(\rho_{700} - \rho_{550})(\rho_{700} / \rho_{670})]}{(1 + 0.16)(\rho_{800} - \rho_{670}) / (\rho_{800} + \rho_{670} + 0.16)}$	B7, B5, B4, B3	(Daughtry et al., 2000; Haboudane et al., 2002; Rondeaux et al., 1996)
MCARI/OSAVI [705,750]	$\frac{[(\rho_{750} - \rho_{705}) - 0.2(\rho_{750} - \rho_{550})(\rho_{750} / \rho_{705})]}{(1 + 0.16)(\rho_{750} - \rho_{705}) / (\rho_{750} + \rho_{705} + 0.16)}$	B6, B5, B3	(Wu et al., 2008)
CI <sub>green</sub>	$\frac{\rho_{NIR}}{\rho_{520-585}} - 1$	B7, B3	(Gitelson et al., 2003, 2006)
CI <sub>red-edge</sub>	$\frac{\rho_{NIR}}{\rho_{695-740}} - 1$	B7, B5	(Gitelson et al., 2003, 2006)

\*NIR refers to near infra-red.

the *in situ* data. For the empirical retrieval models, leave-one-out cross validation procedure was used to evaluate the performance of the VIs, in order to avoid dependence on a single random partitioning of the dataset, and also to guarantee that all samples were used for both training and validation (with each sample used for validation exactly once) (Xie et al., 2016).

## 4. Results

### 4.1. Analysis of Sentinel-2 band configuration and PROSAIL simulation

According to the field measured winter wheat canopy reflectance and Sentinel-2 band positions (Fig. 2), the Sentinel-2 band 3 (542.5–577.5 nm, green band) roughly covers the green peak wavelengths, where reflectance is strongly correlated to chlorophyll content, although Frampton et al (2013) suggested a band width of 525–555 nm would be theoretically optimal for CCC estimation using their datasets. Band 4 (red band) captures the absorption feature due to chlorophyll, which is an important spectral characteristic for vegetation monitoring. A study by Frampton et al. (2013) demonstrated that band 4 is not adversely wide even though it cuts off at 650 nm, as it still captures

most of the chlorophyll absorption in the red region. Bands 5 and 6 offer important information for characterising the sharp increase at the red-edge, and are able to capture more details when compared to previous multispectral satellite data like RapidEye. Band 7, which lies at the beginning of the near infrared region, has been recommended to be the optimal band for capturing near infrared reflectance (Frampton et al., 2013). Taking the above analysis into account, we thus selected bands 2 through 7 and band 8 A for VI calculation. The PROSAIL simulated canopy reflectance was spectrally re-sampled to the Sentinel-2 band configuration.

### 4.2. Optimal spectral indices selection

The coefficient of determination ( $R^2$ ) of the best-fit relationships (Relationships were of various kind for different VIs, including linear and non-linear) between each spectral index and LAI, LCC, and CCC were computed and are presented in Table 4. All VIs were significantly correlated to LAI, LCC and CCC with p values of less than 0.001 except for MCARI/OSAVI. TCARI/OSAVI yielded the highest correlation with LAI and CCC, thus TCARI/OSAVI was used to build the retrieval model for LAI and CCC; whilst TCARI/OSAVI [705,750] yielded the strongest correlation with LCC and then used for LCC retrieval. The fact that, in our study, TCARI/OSAVI was better correlated with LAI and CCC but not with LCC agrees with the principle of the VI, as Haboudane et al. (2002) pointed out that TCARI holds a consistent predictive ability for

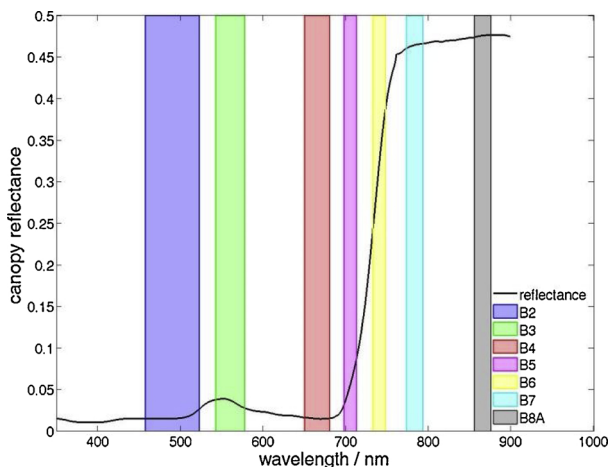


**Fig. 2.** Field measured winter wheat canopy reflectance and indications of Sentinel-2 band positions applied in this study.

**Table 4**  
Coefficient of determination ( $R^2$ ) between each vegetation index and each biophysical variable.

	LAI	LCC	CCC
NDVI	0.55	0.56	0.66
NDRE1	0.58	0.56	0.69
NDRE2	0.64	0.54	0.72
MSR	0.57	0.58	0.71
MTCI	0.62	0.58	0.73
MCARI	0.28	0.42	0.41
TCARI/OSAVI	0.72	0.51	0.78
TCARI/OSAVI [705,750]	0.49	0.63	0.67
MCARI/OSAVI	0.02	0.17	0.10
MCARI/OSAVI [705,750]	0.60	0.47	0.66
CI <sub>green</sub>	0.55	0.59	0.71
CI <sub>red-edge</sub>	0.64	0.59	0.74

canopy chlorophyll estimation, whilst they suggested trying different sets of spectral bands to enhance sensitivity to chlorophyll content variations and reduce response to background and canopy structure effects. Nevertheless, NDRE2, MTCI, and  $CI_{red-edge}$  also had noteworthy results, which agreed with other research conclusions (Dash and Curran, 2004; Frampton et al., 2013). It is worth noting that the red-edge band originally used in the MTCI is based on the MERIS spectral band characteristics, with a spectral bandwidth of 10 nm from 703.75 nm to 713.75 nm. The Sentinel-2 red-edge bands (centred at 705 and 740 nm) are, instead, designed with a spectral bandwidth of 15 nm. Therefore, adaptation of the MTCI formula to specific sensor band characteristics, such as Sentinel-2, might be required. Further investigation is suggested for this issue.

Using the LCC indicative red-edge bands 5 and 6, the estimation power of NDRE1, TCARI/OSAVI [705,750] and MCARI/OSAVI [705,750] increased for LCC, but did not necessarily improve for LAI and CCC, confirming the sensitivity of the red-edge region to LCC (Frampton et al., 2013). For VIs modified with red-edge reflectance, incorporating one red-edge band enhanced relationships with LAI and CCC, but not with LCC. For instance, NDRE2 outperformed NDVI, meanwhile  $CI_{red-edge}$  outperformed  $CI_{green}$  in terms of correlation with LAI and CCC, suggesting that the sharp contrast between near infrared and the beginning of red-edge (which is captured by Band 5 centred at 705 nm) is a strong indication for LAI and CCC.

#### 4.3. Validation of biophysical variables retrieved by RTM and VI approaches

Estimation of LAI, LCC, and CCC was performed with RTMs (ANN and LUT) and VI approaches. For neural network structural parameter, the momentum coefficient (MC) used for final LAI/LCC/CCC retrieval was 0.5/0.8/0.5 respectively, whilst the learning rate (LR) used for final LAI/LCC/CCC retrieval was 0.5/0.1/0.1 respectively. Two hidden layers with five nodes at each layer worked best for our data. The results were validated and plotted against the *in situ* data (62 samples), as shown in Table 5 and Fig. 3. Generally, every approach presented reliable estimates for all investigated biophysical variables with  $R^2$  values of over 0.5 and acceptable RMSE values. For LAI, the highest retrieval accuracy was achieved by TCARI/OSAVI ( $R^2 = 0.68$ , RMSE = 0.94), followed by the ANN method ( $R^2 = 0.50$ , RMSE = 1.35), which had a marginal advantage over the LUT method ( $R^2 = 0.50$ , RMSE = 1.60). In the case of CCC estimation, application of the TCARI/OSAVI obtained comparable accuracy ( $R^2 = 0.71$ , RMSE = 91.22) to the ANN approach ( $R^2 = 0.72$ , RMSE = 108.30), both of which performed better than the LUT approach ( $R^2 = 0.62$ , RMSE = 165.05). As for LCC, the results of the LUT ( $R^2 = 0.71$ , RMSE = 26.92) and the TCARI/OSAVI [705,750] ( $R^2 = 0.61$ , RMSE = 60.75) were highly correlated with measured data but with higher RMSE values than the estimations from the ANN method ( $R^2 = 0.50$ , RMSE = 12.69). The scatter plots in Fig. 3 demonstrate that the biophysical parameters estimated by VIs lie close to the 1:1 line, but significant underestimation and overestimation occurred in the LUT estimations.

By explicit use of all pertinent Sentinel-2 bands during the retrieval, the ANN and LUT methods did not put heavy emphasis on the red region, thus avoiding the saturation that occurred with TCARI/OSAVI

**Table 5**

Validation results of each model for various biophysical variables (n = 62).

	LAI [m <sup>2</sup> /m <sup>2</sup> ]		LCC [μg/cm <sup>2</sup> ]		CCC [μg/cm <sup>2</sup> ]	
	R <sup>2</sup>	RMSE	R <sup>2</sup>	RMSE	R <sup>2</sup>	RMSE
Artificial Neural Network	0.50	1.35	0.50	12.69	0.72	108.30
Look-up-table	0.50	1.60	0.71	26.92	0.62	165.05
TCARI/OSAVI	0.68	0.94	–	–	0.71	91.22
TCARI/OSAVI [705,750]	–	–	0.61	60.75	–	–

when retrieving LAI at high canopy density (LAI > 6). Boochs et al. (1990) pointed out that increases in LCC result in a broadening of the major red absorption feature which causes a shift in the red-edge position (REP) towards longer wavelengths, and also showed that low LCC is associated with a REP close to 700 nm whilst high LCC is associated with a REP near 725 nm. Frampton et al. (2013) produced similar results with a REP of 711–728 nm for LCC values of 16–41 μg/cm<sup>2</sup>. In our case, as LCC increases, the TCARI/OSAVI [705,750] that incorporates Sentinel-2 red-edge bands (bands 5 and 6) reaches saturation for LCC retrieval when LCC > 80 μg/cm<sup>2</sup>, which is likely to be caused by the shifting of the REP due to LCC increasing. A further explanation for the poor retrieval of LCC might be compensations between LAI and LCC, leading to the well-known ill-posed inverse problem (Combal et al., 2003). This is due to the retrieval accuracy of leaf characteristics (e.g. leaf chlorophyll content) from canopy reflectance depends on the strength of the signal transmitted from leaf to canopy level, which is mainly controlled by structural variables such as LAI or leaf angle distribution (Vuolo et al., 2010).

In light of the correlation between the Sentinel-2 data and PROSAIL simulations, the low accuracy of the ANN and LUT methods could be caused by the scattering of Sentinel-2 blue band reflectance, in addition to the small mismatch between the Sentinel-2 red-edge reflectance band and the corresponding PROSAIL simulations. It is possible that enlarging the training dataset (in our case the training dataset consists of 105,300 simulations) may increase the ANN estimation accuracy.

#### 4.4. Validation of biophysical variables retrieved by the SNAP biophysical processor

In order to explore the Sentinel Application Platform (SNAP) biophysical processor for crop biophysical variable retrieval, we used SNAP to retrieve winter wheat LAI and CCC and then compared the results with those retrieved using the ANN, LUT, and VI methods. As we introduced in Section 2.2, SNAP does not deliver LCC retrievals, although some studies have demonstrated that the direct estimation of CCC is more robust and accurate than estimation based on the product of the individual LAI and LCC retrievals (Weiss et al., 2000).

For the 62 field campaign plots in our study, the SNAP biophysical processor obtained LAI and CCC retrieval for 39 plots with good quality (flag = 0). The remaining estimations were discarded due to quality problems. There are different reasons that could cause poor estimations according to the S2 Toolbox Level 2 Product algorithms (Weiss and Baret, 2016), with each represented by a specific flag. In our experiment, poor quality estimations were flagged as having an input out of range (which means that the input values are different from the training data), although in such situations, product values were still provided within the tolerance range. That is to say, SNAP achieved 63% good quality retrievals for our data set. The validation of SNAP estimations is presented in Table 6 and Fig. 4, as well as their corresponding results achieved using the aforementioned RTM and VI approaches. Table 6 and Fig. 4 show that SNAP yielded acceptable accuracy for LAI ( $R^2 = 0.62$ , RMSE = 1.53) and CCC ( $R^2 = 0.53$ , RMSE = 148.58) estimation. In comparison, the VI method remains the most accurate for both LAI ( $R^2 = 0.79$ , RMSE = 0.86) and CCC ( $R^2 = 0.73$ , RMSE = 97.06) estimation, and the scatter plots show that the estimated versus measured values fall close to the 1:1 line.

Similar to the results in Fig. 3, the overestimation and underestimation that occurred in the case of the LUT method as shown in Fig. 4 is likely due to an insufficient training data base. Another reason for the poor estimation of RTM models is the distribution of input parameters, as only when the distribution of training data agrees quite well with the testing data could such an approach give satisfactory estimation results. For example, to prevent underestimations due to many values with low LAI values, we suggest a training data base with increased frequency of LAI below 'saturation' conditions.

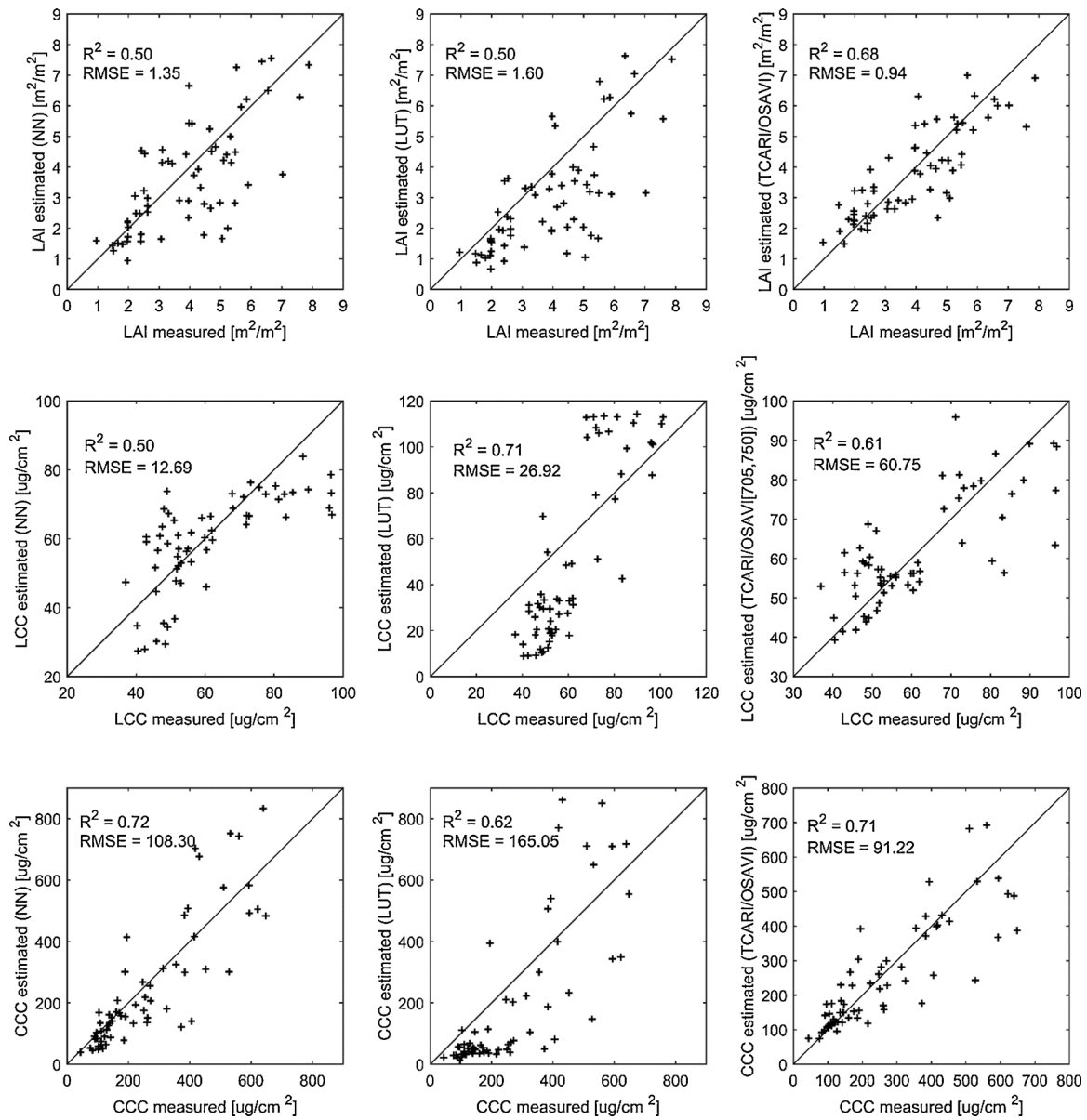


Fig. 3. Estimated versus measured biophysical variables of different retrieval methods (n = 62).

Table 6  
Validation results of SNAP and other model for various biophysical variables (n = 39).

	LAI [m <sup>2</sup> /m <sup>2</sup> ]		CCC [μg/cm <sup>2</sup> ]	
	R <sup>2</sup>	RMSE	R <sup>2</sup>	RMSE
SNAP	0.62	1.53	0.53	148.58
Artificial Neural Network	0.61	1.34	0.75	111.90
Look-up-table	0.60	1.59	0.62	167.55
TCARI/OSAVI	0.79	0.86	0.73	97.06

5. Discussion

In general, VI models provided the most accurate winter wheat biophysical parameter retrievals in our study. The ANN based SNAP biophysical processor provided reliable estimations, although with lower accuracy than the VI methods. The physically based ANN and LUT approaches provided acceptable results but with underestimation and overestimation problems for LCC and CCC retrieval. It should be

noted that the ANN optimized for our dataset did not significantly outperform the SNAP biophysical processor, demonstrating the potential of using SNAP to retrieve winter wheat parameters.

An important issue for the use of the empirical retrieval approach is its limited transferability in the context of various vegetation types and various sites. Since the models are based on *in situ* data, they are only reliable for that specific vegetation type and/or region. Physically based retrieval techniques (e.g. ANN and LUT) are more reliable over multiple sites and crop types. However, RTM parameterization and simulation of training data is time consuming, and improper parameterization may result in poor estimation accuracy. Another drawback of the ANN method is its reduced accessibility, as the algorithm was implemented under the Matlab environment. Fortunately, the gap between ANN algorithms and image processing software has been filled by SNAP. With a pre-trained network, the SNAP biophysical processor performs rather fast in comparison to the ANN and LUT techniques in our study with acceptable accuracy as validated by *in situ* data. Due to the absence of a reliable and regularly updated land cover map at a spatial resolution similar to that of Sentinel-2, no specific ancillary information has been efficiently used in SNAP biophysical processor. The authors of SNAP

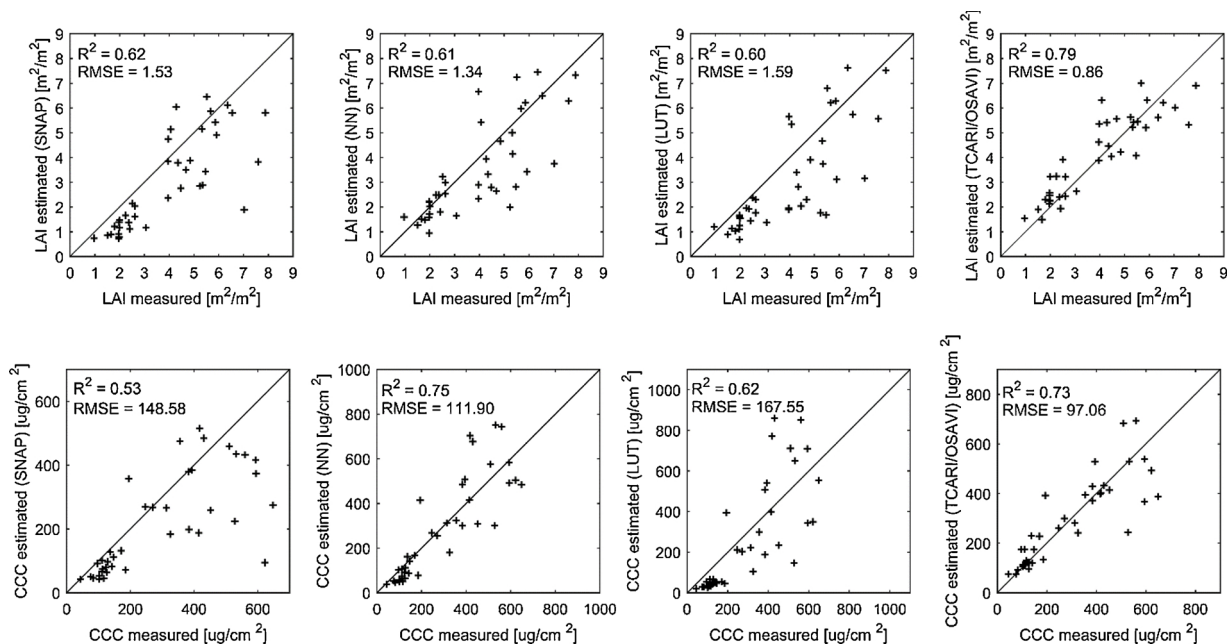


Fig. 4. Estimated versus measured biophysical variables of different retrieval methods (n = 39).

biophysical processor pointed out that SNAP may provide reasonably good estimates over all the cases, but poorer performances as compared to algorithm tailored to a specific surface type (Weiss and Baret, 2016). In our study, SNAP provided less accurate estimations than VI models, but yielded comparable accuracy compared to the ANN and LUT approaches.

One strong assumption embedded in single pixel retrieval algorithms such as those used in this study, is that the pixel targeted belongs to a landscape patch that is homogeneous (at the pixel scale). For any pixel showing strong heterogeneity, such as pixels at the intersection between two different vegetation patches, however, results may be uncertain. This extends also to pixels surrounded by very different neighbouring ones. For such situations, specific algorithms need to be developed.

## 6. Conclusion

This paper focused on evaluating the potential of Sentinel-2 imagery for crop LAI, LCC and CCC estimation with simultaneous application of VIs, ANN and LUT approaches, and particularly the SNAP biophysical processor. Based on field collected winter wheat data and near-synchronous Sentinel-2 images, inversion models were established and validated. The results show that the red-edge bands improved the estimation accuracy of traditional VIs, and the empirical retrieval technique gave the best biophysical variable estimations. But due to its application limitations (crop type and site specificity), we recommend that these methods be used only in small regions or single crop species. The physically based ANN and LUT approaches yielded accuracies second to the empirical models. The SNAP biophysical processor obtained comparable accuracy for LAI and CCC estimation compared to ANN and LUT approaches, in spite of some poor quality estimations flagged by the quality indicator. In conclusion, Sentinel-2 data, especially its red-edge bands, is useful for crop biophysical variable retrieval, and thus has great potential in agricultural applications. SNAP is applicable for winter wheat parameter retrieval, although with lower accuracy than VI models, and fosters the use of rapid physically based approaches with a highly accessible retrieval module embedded directly into the image processing software. The parameter retrieval of a wider range of vegetation is yet to be tested with SNAP.

## Acknowledgements

The authors are very grateful for the financial support provided by National Key R&D Program of China (2016YFB0501501), Technology Development Program of Jilin Province (20180201012GX), and National Natural Science Foundation of China (41871339, 41601466, 41601403). Thanks must also be extended to the editors and reviewers who handled our paper.

## References

- Atzberger, C., 2004. Object-based retrieval of biophysical canopy variables using artificial neural nets and radiative transfer models. *Remote Sens. Environ.* 93 (1), 53–67.
- Bacour, C., Baret, F., Beal, D., 2006. Neural network estimation of LAI, fAPAR, fCover and LAI, from top of canopy MERIS reflectance data: principles and validation. *Remote Sens. Environ.* 105 (4), 313–325.
- Baret, F., Buis, S., 2008. Estimating canopy characteristics from remote sensing observations. Review of methods and associated problems. *Advances in Land Remote Sensing: System, Modeling, Inversion and Application*. pp. 173–201.
- Barnes, E., Clarke, T., Richards, S., Colaizzi, P., Haberland, J., et al., 2000. Coincident detection of crop water stress, nitrogen status and canopy density using ground based multispectral data. Paper Presented at the Proceedings of the 5th International Conference on Precision Agriculture.
- Battude, M., Al Bitar, A., Morin, D., Cros, J., Huc, M., et al., 2016. Estimating maize biomass and yield over large areas using high spatial and temporal resolution Sentinel-2 like remote sensing data. *Remote Sens. Environ.* 184, 668–681. <https://doi.org/10.1016/j.rse.2016.07.030>.
- Boochs, F., Kupfer, G., Dockter, K., Kühbauch, W., 1990. Shape of the red edge as vitality indicator for plants. *Remote Sens.* 11 (10), 1741–1753.
- Campos-Taberner, M., García-Haro, F.J., Camps-Valls, G., Grau-Muedra, G., Nutini, F., et al., 2016. Multitemporal and multiresolution leaf area index retrieval for operational local rice crop monitoring. *Remote Sens. Environ.* 187, 102–118. <https://doi.org/10.1016/j.rse.2016.10.009>.
- Chen, J.M., 1996. Evaluation of vegetation indices and a modified simple ratio for boreal applications. *Can. J. Remote. Sens.* 22 (3), 229–242.
- Claverie, M., Vermote, E.F., Weiss, M., Baret, F., Hagolle, O., et al., 2013. Validation of coarse spatial resolution LAI and FAPAR time series over cropland in southwest France. *Remote Sens. Environ.* 139, 216–230.
- Combal, B., Baret, F., Weiss, M., Trubuil, A., Mace, D., et al., 2003. Retrieval of canopy biophysical variables from bidirectional reflectance: using prior information to solve the ill-posed inverse problem. *Remote Sens. Environ.* 84 (1), 1–15.
- Darvishzadeh, R., Skidmore, A., Schlerf, M., Atzberger, C., 2008a. Inversion of a radiative transfer model for estimating vegetation LAI and chlorophyll in a heterogeneous grassland. *Remote Sens. Environ.* 112 (5), 2592–2604. <https://doi.org/10.1016/j.rse.2007.12.003>.
- Darvishzadeh, R., Skidmore, A., Schlerf, M., Atzberger, C., Corsi, F., et al., 2008b. LAI and chlorophyll estimation for a heterogeneous grassland using hyperspectral measurements. *ISPRS J. Photogramm. Remote. Sens.* 63 (4), 409–426.
- Dash, J., Curran, P.J., 2004. The MERIS terrestrial chlorophyll index. *Int. J. Remote Sens.*

- 25 (23), 5403–5413. <https://doi.org/10.1080/0143116042000274015>.
- Daughtry, C., Walthall, C., Kim, M., De Colstoun, E.B., McMurtrey, J., 2000. Estimating corn leaf chlorophyll concentration from leaf and canopy reflectance. *Remote Sens. Environ.* 74 (2), 229–239.
- Delegido, J., Verrelst, J., Meza, C.M., Rivera, J.P., Alonso, L., et al., 2013. A red-edge spectral index for remote sensing estimation of green LAI over agroecosystems. *Eur. J. Agron.* 46, 42–52. <https://doi.org/10.1016/j.eja.2012.12.001>.
- Duveiller, G., Weiss, M., Baret, F., Defourny, P., 2011. Retrieving wheat green area index during the growing season from optical time series measurements based on neural network radiative transfer inversion. *Remote Sens. Environ.* 115 (3), 887–896. <https://doi.org/10.1016/j.rse.2010.11.016>.
- Feret, J.-B., François, C., Asner, G.P., Gitelson, A.A., Martin, R.E., et al., 2008. PROSPECT-4 and 5: advances in the leaf optical properties model separating photosynthetic pigments. *Remote Sens. Environ.* 112 (6), 3030–3043.
- Feret, J.B., Gitelson, A.A., Noble, S.D., Jacquemoud, S., 2017. PROSPECT-D: towards modeling leaf optical properties through a complete lifecycle. *Remote Sens. Environ.* 193, 204–215. <https://doi.org/10.1016/j.rse.2017.03.004>.
- Frampton, W.J., Dash, J., Watmough, G., Milton, E.J., 2013. Evaluating the capabilities of Sentinel-2 for quantitative estimation of biophysical variables in vegetation. *ISPRS J. Photogramm. Remote. Sens.* 82, 83–92. <https://doi.org/10.1016/j.isprsjprs.2013.04.007>.
- Gao, J., 2006. *Experimental Guidance for Plant Physiology*. China Higher Education Press, Beijing (Chinese) Google Scholar.
- Gitelson, A., Merzlyak, M.N., 1994. Spectral reflectance changes associated with autumn senescence of *Aesculus hippocastanum* L. and *Acer platanoides* L. Leaves. Spectral features and relation to chlorophyll estimation. *J. Plant Physiol.* 143 (3), 286–292.
- Gitelson, A.A., Gritz, Y., Merzlyak, M.N., 2003. Relationships between leaf chlorophyll content and spectral reflectance and algorithms for non-destructive chlorophyll assessment in higher plant leaves. *J. Plant Physiol.* 160 (3), 271–282.
- Gitelson, A.A., Keydan, G.P., Merzlyak, M.N., 2006. Three-band model for noninvasive estimation of chlorophyll, carotenoids, and anthocyanin contents in higher plant leaves. *Geophys. Res. Lett.* 33 (11).
- Green, D.S., Erickson, J.E., Kruger, E.L., 2003. Foliar morphology and canopy nitrogen as predictors of light-use efficiency in terrestrial vegetation. *Agric. For. Meteorol.* 115 (3), 163–171.
- Haboudane, D., Miller, J.R., Tremblay, N., Zarco-Tejada, P.J., Dextraze, L., 2002. Integrated narrow-band vegetation indices for prediction of crop chlorophyll content for application to precision agriculture. *Remote Sens. Environ.* 81 (2–3), 416–426.
- Houlès, V., Mary, B., Machet, J., Guerif, M., Moulin, S., 2001. Do crop characteristics available from remote sensing allow to determine crop nitrogen status. *Proceedings. 2001*; 3. ECPA 2001-06-18-2001-06-20, 917–922.
- Jacquemoud, S., Verhoef, W., Baret, F., Bacour, C., Zarco-Tejada, P.J., et al., 2009. PROSPECT+ SAIL models: a review of use for vegetation characterization. *Remote Sens. Environ.* 113, S56–S66.
- Kira, O., Nguy-Robertson, A.L., Arkebauer, T.J., Linker, R., Gitelson, A.A., 2016. Informative spectral bands for remote green LAI estimation in C3 and C4 crops. *Agric. For. Meteorol.* 218–219, 243–249. <https://doi.org/10.1016/j.agrformet.2015.12.064>.
- Kong, W., Huang, W., Liu, J., Chen, P., Qin, Q., et al., 2017. Estimation of canopy carotenoid content of winter wheat using multi-angle hyperspectral data. *Adv. Space Res.* 60 (9), 1988–2000.
- Kross, A., McNairn, H., Lapen, D., Sunohara, M., Champagne, C., 2015. Assessment of RapidEye vegetation indices for estimation of leaf area index and biomass in corn and soybean crops. *Int. J. Appl. Earth Obs. Geoinf.* 34, 235–248.
- Nguy-Robertson, A., Gitelson, A., Peng, Y., Viña, A., Arkebauer, T., et al., 2012. Green leaf area index estimation in maize and soybean: combining vegetation indices to achieve maximal sensitivity. *Agron. J.* 104 (5), 1336. <https://doi.org/10.2134/agronj2012.0065>.
- Pu, R., Cheng, J., 2015. Mapping forest leaf area index using reflectance and textural information derived from WorldView-2 imagery in a mixed natural forest area in Florida, US. *Int. J. Appl. Earth Obs. Geoinf.* 42, 11–23. <https://doi.org/10.1016/j.jag.2015.05.004>.
- Richter, R., Louis, J., Müller-Wilm, U., 2012. *Sentinel-2 Msi-Level 2a Products Algorithm Theoretical Basis Document 49*. European Space Agency, (Special Publication) ESA SP, pp. 1–72.
- Rondeaux, G., Steven, M., Baret, F., 1996. Optimization of soil-adjusted vegetation indices. *Remote Sens. Environ.* 55 (2), 95–107.
- Rouse Jr, J., Haas, R., Schell, J., Deering, D., 1974. *Monitoring Vegetation Systems in the Great Plains with ERTS 351*. NASA special publication, pp. 309.
- Sims, D.A., Gamon, J.A., 2002. Relationships between leaf pigment content and spectral reflectance across a wide range of species, leaf structures and developmental stages. *Remote Sens. Environ.* 81 (2), 337–354.
- Verhoef, W., 1984. Light scattering by leaf layers with application to canopy reflectance modeling: the SAIL model. *Remote Sens. Environ.* 16 (2), 125–141.
- Verrelst, J., Muñoz, J., Alonso, L., Delegido, J., Rivera, J.P., et al., 2012. Machine learning regression algorithms for biophysical parameter retrieval: opportunities for Sentinel-2 and -3. *Remote Sens. Environ.* 118, 127–139. <https://doi.org/10.1016/j.rse.2011.11.002>.
- Verrelst, J., Rivera, J.P., Leonenko, G., Alonso, L., Moreno, J., 2014. Optimizing LUT-Based RTM Inversion for Semiautomatic Mapping of Crop Biophysical Parameters from Sentinel 2 and 3 Data Role of Cost Functions. *IEEE Trans. Geosci. Remote. Sens.* 52 (1), 257–267.
- Verrelst, J., Camps-Valls, G., Muñoz-Marí, J., Rivera, J.P., Veroustraete, F., et al., 2015a. Optical remote sensing and the retrieval of terrestrial vegetation bio-geophysical properties – a review. *ISPRS J. Photogramm. Remote. Sens.* 108, 273–290. <https://doi.org/10.1016/j.isprsjprs.2015.05.005>.
- Verrelst, J., Rivera, J.P., Veroustraete, F., Muñoz-Marí, J., Clevers, J.G.P.W., et al., 2015b. Experimental sentinel-2 LAI estimation using parametric, non-parametric and physical retrieval methods – a comparison. *ISPRS J. Photogramm. Remote. Sens.* 108, 260–272. <https://doi.org/10.1016/j.isprsjprs.2015.04.013>.
- Viña, A., Gitelson, A.A., Nguy-Robertson, A.L., Peng, Y., 2011. Comparison of different vegetation indices for the remote assessment of green leaf area index of crops. *Remote Sens. Environ.* 115 (12), 3468–3478.
- Vuolo, F., Atzberger, C., Ritcher, K., D'Urso, G., Dash, J., 2010. Retrieval of biophysical vegetation products from rapideye. *ISPRS Symposium. XXXVIII(7A)*.
- Weiss, M., Baret, F., 2016. S2ToolBox Level 2 products: LAI, FAPAR, FCOVER, Version 1.1. In *ESA Contract n° 4000110612/14/I-BG* (p. 52): INRA Avignon, France.
- Weiss, M., Baret, F., Myneni, R., Pragnère, A., Knyazikhin, Y., 2000. Investigation of a model inversion technique to estimate canopy biophysical variables from spectral and directional reflectance data. *Agronomie* 20 (1), 3–22.
- Wu, C., Niu, Z., Tang, Q., Huang, W., 2008. Estimating chlorophyll content from hyperspectral vegetation indices: modeling and validation. *Agric. For. Meteorol.* 148 (8–9), 1230–1241. <https://doi.org/10.1016/j.agrformet.2008.03.005>.
- Xie, Q., Huang, W., Liang, D., Chen, P., Wu, C., et al., 2014. Leaf area index estimation using vegetation indices derived from airborne hyperspectral images in winter wheat. *IEEE J. Sel. Top. Appl. Earth Obs. Remote. Sens.* 7 (8), 3586–3594.
- Xie, Q., Huang, W., Zhang, B., Chen, P., Song, X., et al., 2016. Estimating winter wheat leaf area index from ground and hyperspectral observations using vegetation indices. *IEEE J. Sel. Top. Appl. Earth Obs. Remote. Sens.* 9 (2), 771–780.